

1
2
3
4
5
6
7
8
9
10
11
12
13
14
15
16

SUPPLEMENTAL FIGURES AND TABLES

Molecular pathology and cystogenic propensity of the ADPKD Taiwan founder variant

Authors and affiliations:

Louise F. Kimura^{1*}, Orhi Esarte Palomero^{1*}, Megan Larmore¹, Paul G. DeCaen^{1,2**}, Thuy N. Vien^{1**}

1) Department of Pharmacology, Feinberg School of Medicine, Northwestern University, Chicago, Illinois, USA.

2) Chemistry of Life Processes Institute, Northwestern University, Evanston, Illinois, USA

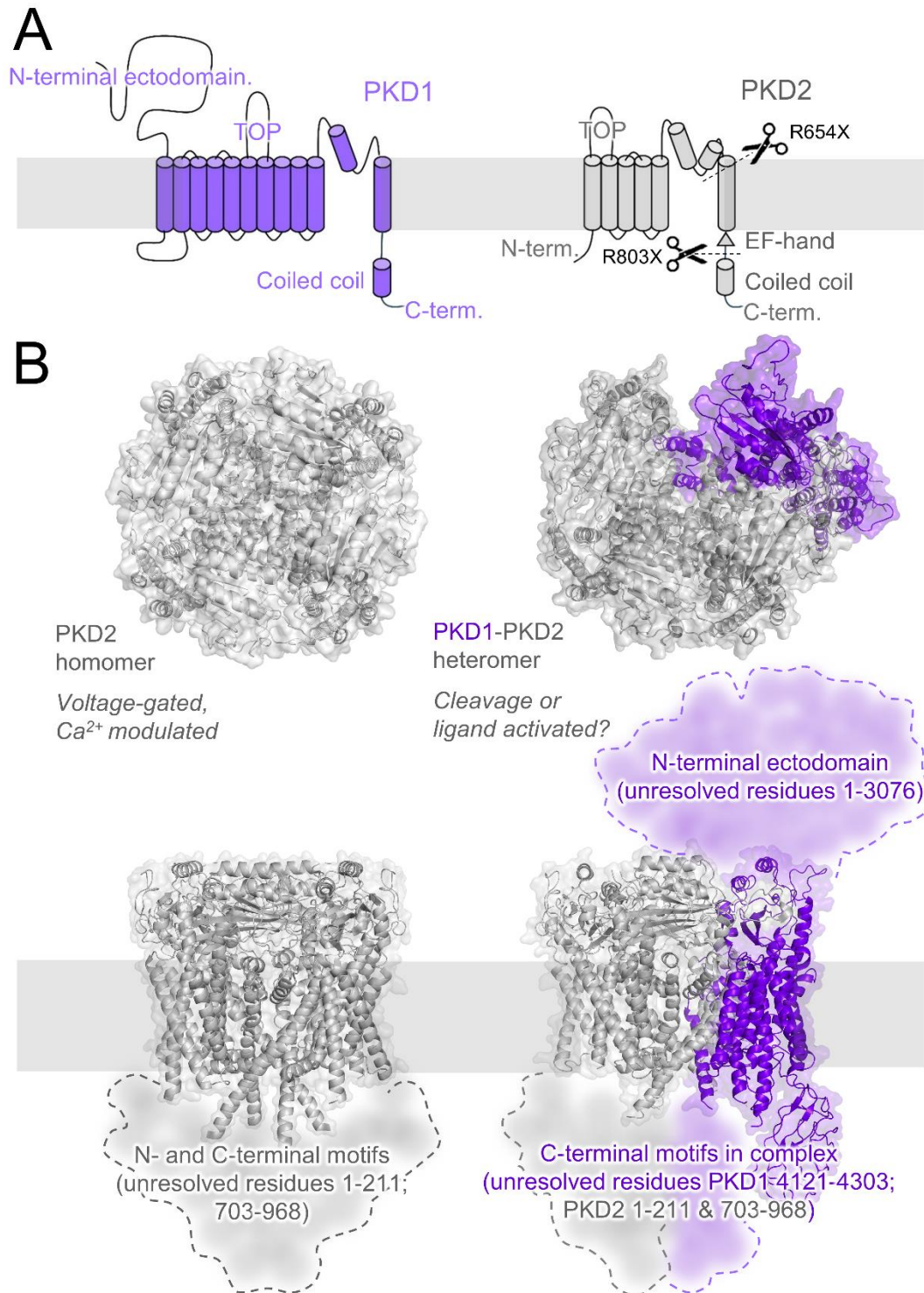
*Authors contributed equally to this work.

**Corresponding authors.

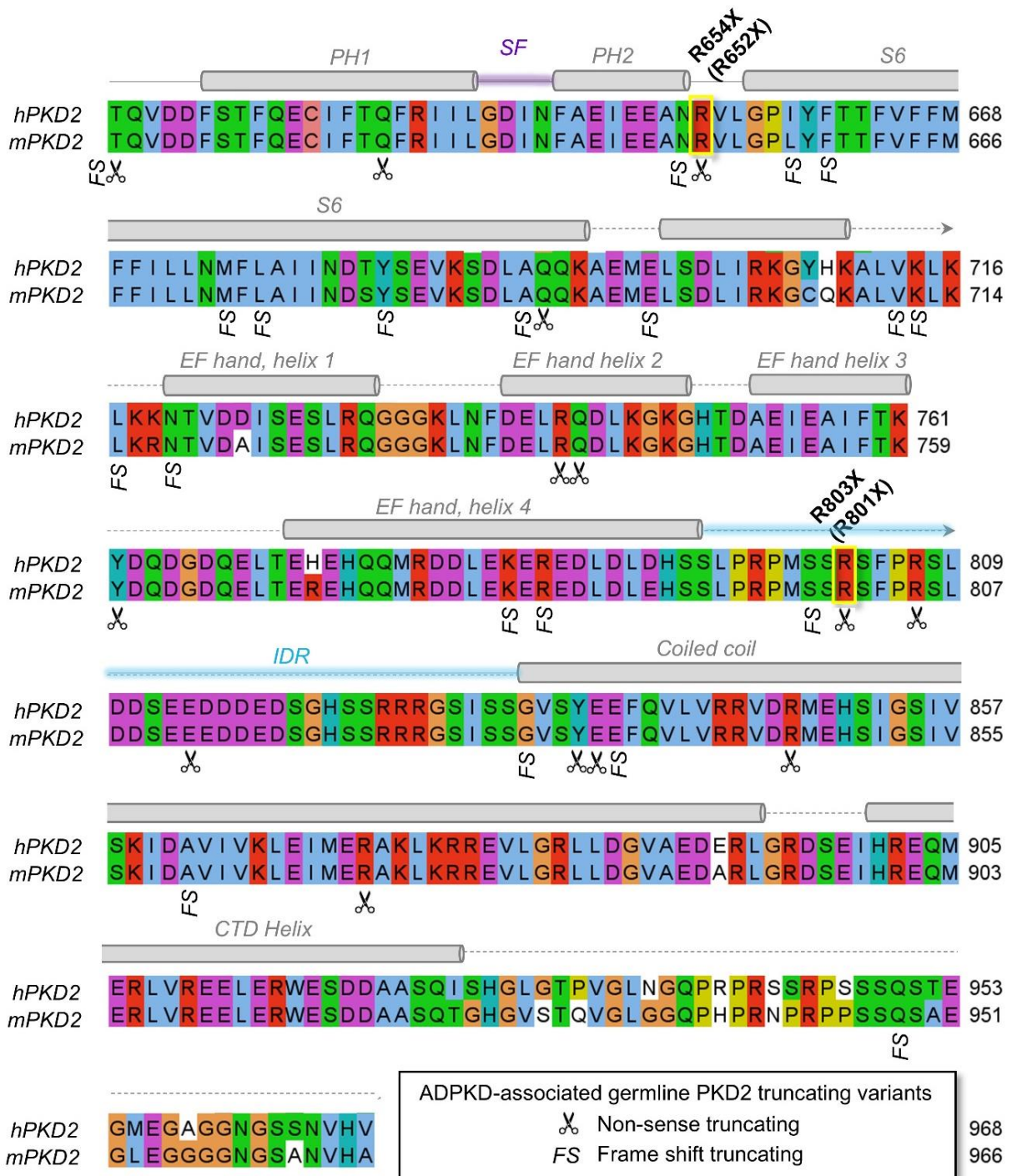
Corresponding authors contact information.

Paul G DeCaen, 320 East Superior, Chicago IL 60601; 206-403-8811; paul.decaen@northwestern.edu

Thuy N. Vien, 320 East Superior, Chicago IL 60601; 206-854-9450; thuy.vien@northwestern.edu



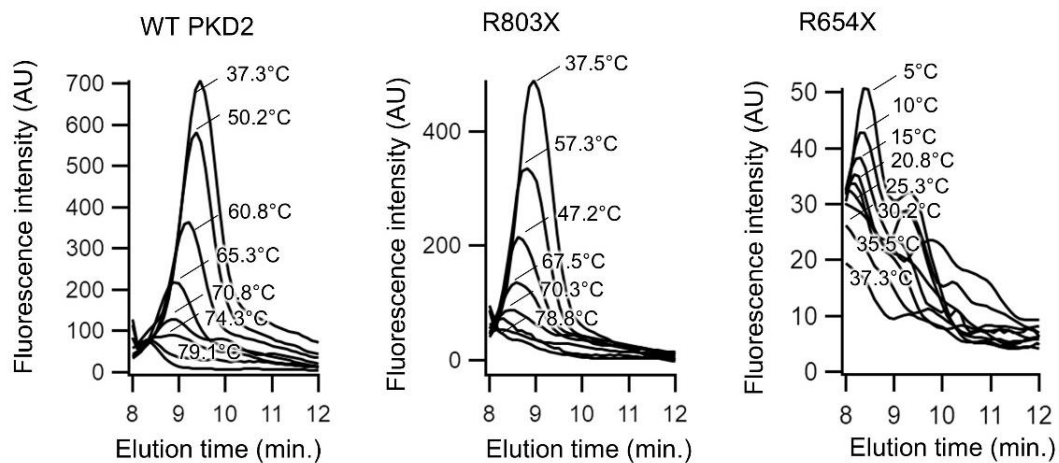
18 **Supplemental Figure 1. PKD2 may form homomeric or heteromeric ion channel complexes.** A) topology of
 19 PKD1 and PKD2 polycystin channel subunits. B) Cryo-EM structures of voltage-gated, calcium modulated
 20 homomeric PKD2 (PDB ID: 5T4D) channel and putative ligand or cleavage activated PKD1-PKD2 (PDB ID: 6A70)
 21 channel complex(1, 2). Top row images are external views and bottom row images are transmembrane views of
 22 the channel structures. Note the large portions of the channels which are structurally unresolved.



23

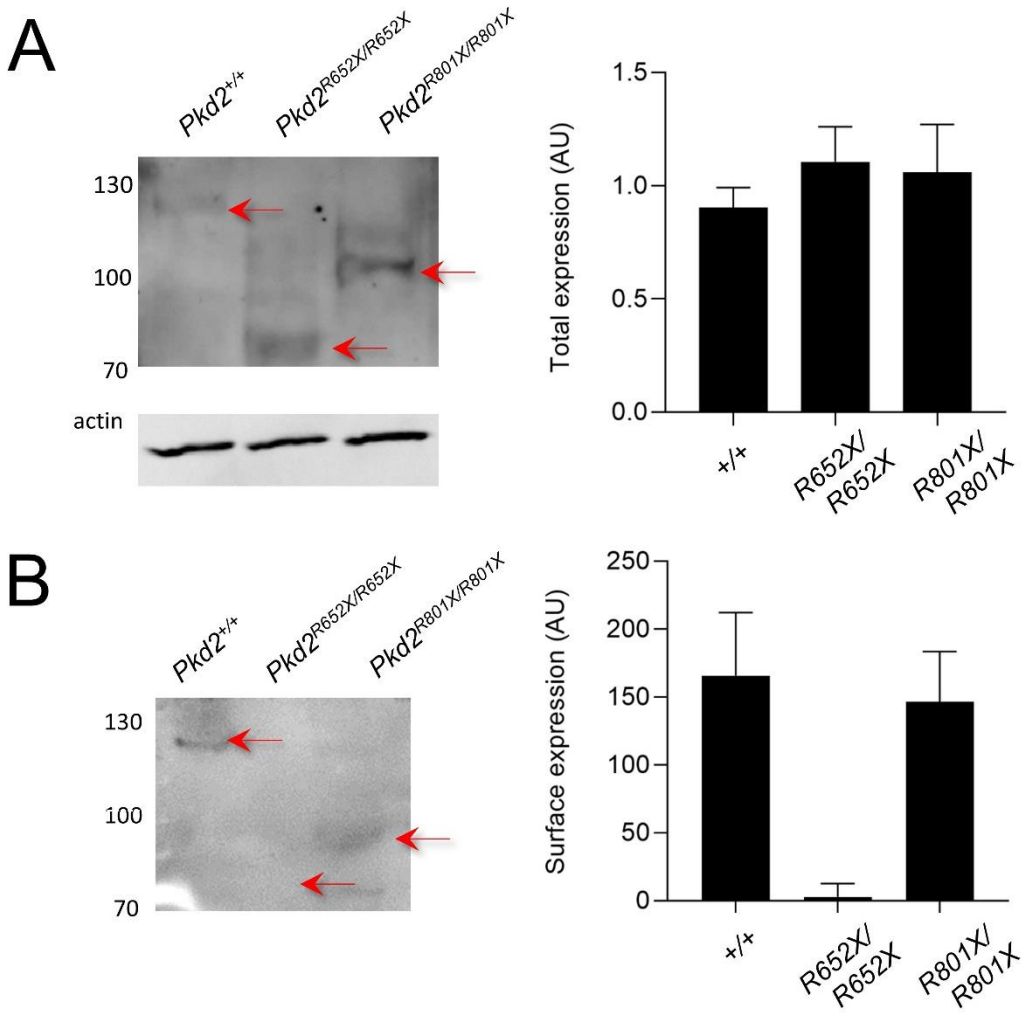
24

25 **Supplemental Figure 2. Location of ADPKD-associated truncating variants.** C-terminal amino acid Clustal-
 26 omega alignment of human and mouse PKD2 rendered in JalView applying the default color scheme: Hydrophobic
 27 (blue); polar (green); glutamate, aspartate (purple). Special amino acids are designated with their own color: glycine
 28 (orange); proline (yellow) and tyrosine or histidine (cyan). The barrels indicate alpha helices found in the PKD2
 29 AlphaFold3 structures and the location of ADPKD-associated truncating variants (non-sense, frameshift) are
 30 indicated(3).
 31



33 **Supplemental Figure 3. PKD2 R654X variant destabilizes channel assembly.** Thermal denature profiles (T=
 34 4-80°C) for WT and truncating variant channel. Peak homomeric tetramer elution times were observed 8-10
 35 minutes. A clear thermal transition temperature was less obvious for the R654X variant.

36



38 **Supplemental Figure 4. Total and surface expression of endogenous PKD2 and truncation variants.** **A)** Left,
39 western blot of total PKD2 protein harvested from homozygous mice expressing WT (*Pkd2*^{+/+}) or truncation variant
40 (*Pkd2*^{R652X/R652X}, *Pkd2*^{R801X/R801X}) alleles. Right, protein expression as determined anti-PKD2 monoclonal (Sigma
41 Aldrich, WH0005311M1), secondary anti-IgG rabbit (DyLight 488 1:5000) signal intensity normalized to anti-actin
42 protein loading control (MA5-15739, Invitrogen 1:5000). **B)** Biotinylation plots detecting surface expression of PKD2
43 and relative abundance. N= 4 blots from renal tissue harvested from 4 embryonic mice per genotype.
44

Channel	Unitary Conductance	$V_{1/2}$ [Ca ²⁺] _{in} = 100 nM	$V_{1/2}$ [Ca ²⁺] _{in} = 30 μ M	$\Delta V_{1/2}$
PKD2, WT	97 \pm 3 pS	69 mV \pm 7	18 mV \pm 7	-51 mV
PKD2, R803X	95 \pm 3 pS	72 mV \pm 8	23 mV \pm 8	-49 mV

46 **Supplemental Table 1. Gating properties of PKD2 ADPKD variants.** Boltzmann parameters ($V_{1/2}$) and (Z)
 47 resulting from fitting the voltage-dependent opening relationship of PKD2 channels reported in Figure 3 and
 48 Supplemental Figure 3. Error is equal to S.D.

49

50

Genotype	lateral renal cysts	bilateral renal cysts	liver cysts
<i>Pkd2</i> ^{+/R652X}	25% (3/12)	8% (1/12)	8% (1/12)
<i>Pkd2</i> ^{+/R801X}	11% (2/14)	0% (0/14)	0% (0/14)
<i>Pkd2</i> ^{+/fl} Control	0%, (0/14)	0%, (0/14)	0%, (0/14)
<i>Pkd2</i> ^{+/fl} Doxycycline	14%, (2/14)	0%, (0/14)	7%(1/14)
<i>Pkd2</i> ^{R652X/fl} Control	28% (2/7)	14% (1/7)	14% (1/7)
<i>Pkd2</i> ^{R652X/fl} Doxycycline	All bilateral	100%, (5/5)	20% (1/5)
<i>Pkd2</i> ^{R801X/fl} Control	28% (2/7)	0% (0/7)	14% (1/7)
<i>Pkd2</i> ^{R801X/fl} Doxycycline	All bilateral	100%, (7/7)	14%(1/7)

51 **Supplemental Table 2. Histological features of mice expressing ADPKD variants.** Incidence of renal (lateral,
 52 bilateral) and liver cysts for each murine genotype.

53

54

55 **REFERENCES**

- 56 1. Shen PS, Yang X, DeCaen PG, Liu X, Bulkley D, Clapham DE, et al. The Structure of the Polycystic Kidney
57 Disease Channel PKD2 in Lipid Nanodiscs. *Cell*. 2016;167(3):763-73 e11.
- 58 2. Su Q, Hu F, Ge X, Lei J, Yu S, Wang T, et al. Structure of the human PKD1-PKD2 complex. *Science*.
59 2018;361(6406).
- 60 3. Waterhouse AM, Procter JB, Martin DM, Clamp M, and Barton GJ. Jalview Version 2--a multiple sequence
61 alignment editor and analysis workbench. *Bioinformatics*. 2009;25(9):1189-91.

62